Received: 1 July 2022 | Revised: 14 February 2023 | Accepted: 15 February 2023

DOI: 10.1111/gcb.16643

Global Change Biology WILEY

RESEARCH ARTICLE

Across-model spread and shrinking in predicting peatland carbon dynamics under global change

Enqing Hou[1,2] | Shuang Ma[1,3] | Yuanyuan Huang[4] | Yu Zhou[1,5] | Hyung-Sub Kim[6] | Efrén López-Blanco[7,8] | Lifen Jiang[1] | Jianyang Xia[9] | Feng Tao[10] | Christopher Williams[5] | Mathew Williams[11] | Daniel Ricciuto[12] | Paul J. Hanson[12] | Yiqi Luo[13]

[1]Center for Ecosystem Science and Society, Northern Arizona University, Flagstaff, Arizona, USA

[2]Key Laboratory of Vegetation Restoration and Management of Degraded Ecosystems, South China Botanical Garden, Chinese Academy of Sciences, Guangzhou, China

[3]Jet Propulsion Laboratory, California Institute of Technology, Pasadena, California, USA

[4]CSIRO Oceans and Atmosphere, Aspendale, Victoria, Australia

[5]Graduate School of Geography, Clark University, Worcester, Massachusetts, USA

[6]Department of Environmental Science and Ecological Engineering, Korea University, Seoul, South Korea

[7]Department of Ecoscience, Arctic Research Centre, Aarhus University, Roskilde, Denmark

[8]Department of Environment and Minerals, Greenland Institute of Natural Resources, Nuuk, Greenland

[9]Research Center for Global Change and Complex Ecosystems, School of Ecological and Environmental Sciences, East China Normal University, Shanghai, China

[10]Ministry of Education Key Laboratory for Earth System Modeling, Department of Earth System Science, Tsinghua University, Beijing, China

[11]School of GeoSciences, University of Edinburgh, Edinburgh, UK

[12]Environmental Sciences Division, Oak Ridge National Laboratory, Oak Ridge, Tennessee, USA

[13]School of Integrative Plant Science, Cornell University, Ithaca, New York, USA

Correspondence
Enqing Hou, Key Laboratory of Vegetation Restoration and Management of Degraded Ecosystems, South China Botanical Garden, Chinese Academy of Sciences, Guangzhou 510650, China.
Email: houeq@scbg.ac.cn

Yiqi Luo, School of Integrative Plant Science, Cornell University, Ithaca, NY 14853, USA.
Email: yl2735@cornell.edu

Funding information
DOE, Office of Science, Office of Biological and Environmental Research; European Union's HORIZON research and innovation program, Grant/Award Number: 101056921; Guangdong Basic and Applied Basic Research Foundation, Grant/Award Number: 2022B1515020014; National Natural Science Foundation of China, Grant/Award Number: 32271644 and 31870464; National Research Foundation of Korea, Grant/Award

Abstract

Large across-model spread in simulating land carbon (C) dynamics has been ubiquitously demonstrated in model intercomparison projects (MIPs), and became a major impediment in advancing climate change prediction. Thus, it is imperative to identify underlying sources of the spread. Here, we used a novel matrix approach to analytically pin down the sources of across-model spread in transient peatland C dynamics in response to a factorial combination of two atmospheric CO_2 levels and five temperature levels. We developed a matrix-based MIP by converting the C cycle module of eight land models (i.e., TEM, CENTURY4, DALEC2, TECO, FBDC, CASA, CLM4.5 and ORCHIDEE) into eight matrix models. While the model average of ecosystem C storage was comparable to the measurement, the simulation differed largely among models, mainly due to inter-model difference in baseline C residence time. Models generally overestimated net ecosystem production (NEP), with a large spread that was mainly attributed to inter-model difference in environmental scalar. Based on the sources of spreads identified, we sequentially standardized model parameters to shrink simulated ecosystem C storage and NEP to almost none. Models generally

Number: NRF-2018R1A2B6001012; National Science Foundation Grant DEB, Grant/Award Number: 1655499 and 2017884; Oak Ridge National Laboratory, Grant/Award Number: 4000158404; US Department of Energy (DOE), Grant/Award Number: DE-SC0020227 and DE-AC05-00OR22725

captured the observed negative response of NEP to warming, but differed largely in the magnitude of response, due to differences in baseline C residence time and temperature sensitivity of decomposition. While there was a lack of response of NEP to elevated CO_2 (eCO_2) concentrations in the measurements, simulated NEP responded positively to eCO_2 concentrations in most models, due to the positive responses of simulated net primary production. Our study used one case study in Minnesota peatland to demonstrate that the sources of across-model spreads in simulating transient C dynamics can be precisely traced to model structures and parameters, regardless of their complexity, given the protocol that all the matrix models were driven by the same gross primary production and environmental variables.

KEYWORDS
across-model spread, carbon residence time, environmental scalar, land carbon dynamics, matrix model, SPRUCE experiment, traceability analysis

1 | INTRODUCTION

Earth system models (ESMs) is a primary tool for predicting the global carbon (C) cycle and informing climate change mitigation policies (IPCC, 2021). However, ESMs have yielded large across-model spread in the predicted global C cycle, which primarily arises from the land C component, as shown in the fourth to sixth assessment reports of the Intergovernmental Panel on Climate Change (IPCC; Ciais et al., 2013; Friedlingstein et al., 2006; J. Zhou et al., 2021). Generally, most land models of ESMs represent land C input via photosynthesis, transformations among multiple pools, and losses via plant autotrophic and microbial heterotrophic respiration (Luo et al., 2016; Manzoni & Porporato, 2009). However, there are large differences in model parameters, the number of C pools, and the functions to represent responses of C cycling processes to temperature and moisture (Koven et al., 2013; Luo et al., 2016). These differences result in land models with distinct structures and varying complexities (Bradford et al., 2016; Manzoni & Porporato, 2009), making it a growing challenge to understand across-model spread in simulated land C dynamics. Thus, understanding across-model spread is urgently needed to facilitate the development of the next generation of land models (IPCC, 2021).

Several methods have been developed to analyze and reduce across-model spread or model uncertainty (i.e., uncertainty shown in a single model) in simulating land C dynamics, such as benchmarking, sensitivity analysis, reduced complexity model, model intercomparison, and data assimilation (Huntzinger et al., 2017; Keenan & Williams, 2018; López-Blanco et al., 2019; Luo et al., 2012, 2016; Todd-Brown et al., 2013; Wieder et al., 2015). For example, benchmarking analysis can quantitatively assess model fidelity through rigorous comparisons with measurements and observations (Collier et al., 2018; Luo et al., 2012). Sensitivity analysis provides information on the importance of variables, parameters, and other inputs on model uncertainty (Huang, Zhu, et al., 2018). Model intercomparison can disentangle, interpret, and inform understanding of across-model spread (Huntzinger et al., 2013, 2017). Data assimilation can rigorously integrate model and data to reduce model uncertainty (Luo et al., 2016). All these methods are fundamental to understand and reduce model uncertainty or across-model spread in land C dynamics. However, these methods have been applied unevenly among models due to required technical efforts and computational costs, and none of them enables a systematical and analytical analysis of across-model spread (Keenan & Williams, 2018; J. Zhou et al., 2021).

Recently, a matrix approach has been developed to unify different land C models and analytically understand model uncertainty or across-model spread (Luo et al., 2017, 2022). The matrix approach is based on the fact that although hundreds of models have been developed to represent land C dynamics (Manzoni & Porporato, 2009), the current generation of land C models inside ESMs all use multiple pools to represent various land C compartments and transfers among them (Luo et al., 2016; Sierra et al., 2018). This common structure makes it possible to unify the land C models in a matrix form, by accommodating any number of pools, and by folding all C cycling processes into the terms of the matrix equation related to C input, C allocation into different plant organs, C turnover rate and its environmental modifier, and C transfers among pools (Luo et al., 2016). This unification enables an analytical analysis of sources of model uncertainty or across-model spread using a traceability framework in a hierarchal way (Luo et al., 2017; Xia et al., 2013; J. Zhou et al., 2021; S. Zhou et al., 2018). This framework has been used to analyze across-model spread in C simulations in steady states (Rafique et al., 2016; Wei et al., 2022; Xia et al., 2013) and has also been expanded to analyze sources of uncertainty in ecosystem C storage in non-steady states simulated by a single model (Jiang et al., 2017; Luo et al., 2017). However, the framework has yet been used to pin down the sources of the across-model spread in transient ecosystem C simulations under global change. In fact, C cycling in most, if not all, terrestrial ecosystems are in dynamic disequilibrium states, due to the prevalence of global change (e.g., elevated CO_2 [eCO_2] and climate warming) and disturbance (e.g., deforestation

and fire) over the land (Luo & Weng, 2011). Thus, it is a high priority to pin down sources of the across-model spread in transient C dynamics in non-steady states.

Peatlands contribute disproportionately to the long-term storage of terrestrial C, with those at high latitudes especially vulnerable to climate change, and thus may have important C cycle feedbacks to the atmosphere with global climate implications (Hanson et al., 2020; Lopez-Blanco et al., 2022; Nichols & Peteet, 2019). The responses of these ecosystems to global change have been explored by more and more manipulative experiments (Bridgham et al., 2008; Huang et al., 2021), among which the Spruce and Peatland Responses Under Changing Environments (SPRUCE) experiment is a unique one (Hanson et al., 2020). The SPRUCE experiment is an ecosystem-level climate change manipulation that focuses on the whole-ecosystem responses to multiple levels of warming at both ambient and eCO_2 concentration (Hanson et al., 2016, 2017, 2020). It is unique in the size of the plots (114 m^2 for each enclosure) that enclosed intact examples of ombrotrophic boreal bogs, and covers a larger range (+0 to +9°C) of warming treatments than other peatland experiments (≤5°C). The estimates of ecosystem-level annual C budget from the experiment provide a unique opportunity to examine model performance in capturing the nature of observed ecosystem responses to climate change manipulations. Earlier versions of the ELM-SPRUCE model have been used to analyze model uncertainty of net ecosystem production (NEP) simulation at the site, and those simulations indicated relatively modest NEP responses to warming (Griffiths et al., 2017). An updated version of ELM-SPRUCE, mainly by adding phosphorus cycling, C and nutrient storage pools, and improving phenology, captured the negative responses of NEP to warming in field but failed to predict the lack of observable response to eCO_2 (Hanson et al., 2020). Moreover, while observed temperature sensitivity of NEP did not differ between ambient CO_2 and eCO_2, simulated temperature sensitivity reduced under eCO_2 compared with ambient CO_2 (Hanson et al., 2020). However, reasons for the model-data mismatches and whether other land C models perform similar as the ELM-SPRUCE in simulating peatland C responses to global change remain unclear.

As part of the SPRUCE effort, this study aimed to examine across-model spread in transient C storage under global change manipulations and, meanwhile, pin down its sources analytically using the matrix approach. We firstly converted the C cycle module of eight land surface models into eight matrix models. The eight matrix models differ largely in complexity, with the number of C pools ranging from 2 to 101. We then used the matrix models to simulate ecosystem C dynamics and compared the simulations to the observations in the SPRUCE experiment. Since our matrix models were not embedded in the original models (i.e., run in standalone), we cannot explore across-model spread in gross primary production (GPP). Therefore, we deliberately used the same GPP and environmental variables (e.g., soil temperature and water content) in each treatment to drive all models, to focus this study on the allocation, transfer, and turnover processes of C. Finally, we analyzed the sources of the across-model spread in transient C dynamics using both backward and forward analyses. The backward analysis is a transient traceability analysis, which can trace the source of spread back to its components hierarchically (Jiang et al., 2017; Luo et al., 2017; J. Zhou et al., 2021). The forward analysis is via parameter manipulation, in which we manipulated parameters in the matrix models to investigate their contributions to spread. While the backward analysis is to partition sources of spread, the forward analysis can explore the role of each parameter in causing the across-model spread. Our analyses demonstrate that consolidating multiple land C models into a unified matrix form enables an analytical and systematical examination of the across-model spread in transient peatland C dynamics under global change to pin down its sources, which is a step forward for understanding the sources of the across-model spread from model intercomparison projects (MIPs) in comparison with the previous studies.

2 | METHODS

2.1 | Study site and experimental treatments

The experiment selected in this study was the SPRUCE experiment in the S1 bog in the Marcell Experimental Forest in northern Minnesota, USA (Latitude 47.503 N, Longitude 93.483 W). The experiment was selected mainly for two reasons. First, it is still a challenge to simulate C dynamics in peatlands, given the small living biomass relative to the amount of soil organic matter, the difficulty to simulate peatland hydrology that is closely tied to the humification of the peat file, and the relatively slow turnover rates of plant tissues and dead organic matter than those in other ecosystems (e.g., temperate forests). Second, the global change experiment (two atmospheric CO_2 levels × five warming levels) at the SPRUCE is unique in that, the treatments utilized plot (114 m^2 for each enclosure) enclosed intact examples of ombrotrophic boreal bogs that contained the diversity of the natural ecosystem (tree, shrubs, mosses, microbes, and a deep peat soil), and the warming treatment covers a larger range of warming (+0 to +9°C) than other warming experiments in peatlands (Hanson et al., 2020).

The overstory vegetation of the S1 bog is dominated by two tree species: *Picea mariana* and *Larix laricina*, underlain by a bryophyte layer dominated by *Sphagnum* spp. mosses (Hanson et al., 2020). Mean annual temperature and precipitation at the site are approximately 3°C and 770 mm, respectively (Hanson et al., 2017). In the experiment, the two atmospheric CO_2 levels are ambient (~400 ppm) and eCO_2 (900 ppm) concentrations, respectively; the five warming levels are whole-ecosystem warming by +0, +2.25, +4.5, +6.75, and +9°C, respectively; another two ambient treatment plots without an enclosure were not considered in this study (Hanson et al., 2020). The environmental changes were experimentally created using a regression-based experimental design, with one 12.8-m diameter × 7-m tall, open-top enclosure per treatment (Hanson et al., 2020). Whole-ecosystem warming began in August 2015 following a year of belowground-only warming, which commenced in 2014. The

eCO_2 treatment was initiated in June 2016. Carbon dynamics in this peatland have been measured since 2011, that is, 3–4 years ahead of the treatments (Hanson et al., 2016, 2017). Therefore, simulations in this study started in 2011. Detailed site description and experiment design were described previously by Hanson et al. (2017, 2020).

2.2 | Model conversion and parameterization

The C cycle modules of eight land models were converted into eight matrix C models than run in standalone. The eight land models are the Terrestrial Ecosystem Model (TEM; Raich et al., 1991), Data Assimilation Linked Ecosystem Carbon model version 2 (DALEC2; Bloom & Williams, 2015), Terrestrial ECOsystem (TECO) model (Luo et al., 2017), Forest Biomass and Dead organic matter Carbon (FBDC, previously known as KFSC) model (Lee et al., 2014), Carnegie-Ames-Stanford approach biosphere (CASA) model (Potter et al., 1993), CENTURY version 4 on forest ecosystem (Kirschbaum & Paul, 2002), Community Land Model Version 4.5 (CLM4.5) (Huang, Lu, et al., 2018), and Organizing Carbon and Hydrology in Dynamic Ecosystems (ORCHIDEE) model (Huang, Zhu, et al., 2018) (Table S1). These models were selected by the authors who participated in a model conversion working group organized during the 2nd Training Course on New Advances in Land Carbon Cycle Modeling (https://www2.nau.edu/luo-lab/?training_course_2019), based on the authors' modeling experiences.

While the list of our models is not a comprehensive one, it includes eight models with a range of complexity (the number of C pools ranging from 2 to 101), which represent the land C models used in the current generation of ESMs well (Wei et al., 2022). For simplicity, the abbreviations of the original models are used to represent their C cycle modules in the matrix forms (i.e., the matrix models) as well, unless otherwise specified. The original FBDC runs yearly, but the matrix-based FBDC runs daily. Other matrix models run in the same time steps as the original models, that is, the TEM, CASA and CENTURY4 run monthly, and the DALEC2, TECO, CLM4.5 and ORCHIDEE run daily. Here, we provide a condensed description of the model conversion, full details can be found in Text S1.

In all the eight models, C enters ecosystem as GPP or net primary production (NPP), transfers among compartments, and loses via autotrophic or heterotrophic respiration based on first-order kinetics (Figure 1). Given this similarity, all the models were converted into the following matrix form:

$$\frac{dX(t)}{dt} = \beta(t)B \times u(t) - (A\xi(t)K + V) \times X(t), \quad (1)$$

where the left part (i.e., the part before the equal symbol) depicts C change rate, and the right part depicts the difference between C input rate (the component before the minus symbol) and C output rate (the component after the minus symbol) at time t. $X(t)$ indicates C pool size at time t, $dX(t)$ indicates change in C pool size, dt indicates change in time, $u(t)$ indicates C input through photosynthesis (i.e., GPP here). B indicates time-averaged coefficients of C allocation from GPP to plant tissues, and $\beta(t)$ indicates the modifier of B at time t; the multiplication of B and $\beta(t)$ represents C allocation coefficients at time t; sum of the multiplication across all cells indicates plant C use efficiency (CUE) at time t. K is a matrix of baseline C turnover rates, which indicate the baseline rates of C leaving individual pools through mortality or decomposition. A is a matrix of transfer coefficients, which indicate C transfer in the network of multiple interconnected pools. V is a matrix of vertical transfer coefficients, which indicate the rates of C mixing across layers in a soil profile. $\xi(t)$ indicates the scalar depicting environmental modification of the K matrix, and can be further calculated as follows:

$$\xi(t) = \xi_T(t)\xi_W(t)\xi_O(t), \quad (2)$$

where $\xi_T(t), \xi_W(t), \xi_O(t)$ indicate the scalars depicting the modifications by temperature, water, and other environmental factors (e.g., oxygen), respectively, at time t. Values in the matrices are indicated by the corresponding lowercases, for example, a value in the K matrix is indicated by k.

It is too time consuming to convert traditional C cycle modules into a unified matrix form and embed the matrix version of modules in the eight original models by this single study. Therefore, we converted the eight traditional C cycle modules into eight matrix-based C models that can run in standalone, by directly extracting the above coefficients from each of the eight land models. Whenever the coefficients depend on plant or soil properties, they were estimated using the plant or soil properties at the SPRUCE site or sites with similar vegetation or soil types (Text S1). During the extraction, some simplifications were made, mainly of using fixed GPP and time constant C allocation coefficients. This is because that GPP and C allocation coefficients usually depend on plant phenology, nutrient availability, and downstream values (e.g., leaf biomass), which are difficult to be represented in a matrix form. How these model simplifications may affect our results were explored by sensitivity analyses following.

Carbon allocation coefficients vary with time in the original TEM, TECO, CLM4.5, and ORCHIDEE, depending on variables such as air temperature, soil water content, and maximum plant growth rate; their approximate time averages were used in the matrix forms. Specifically, an observed plant CUE in a boreal conifer forest (0.4) in McGuire et al. (1992) was used as $b1$ in the matrix-based TEM. Empirical constant C allocation coefficients in Luo et al. (2017) were directly used in the matrix-based TECO. Since plant C modules in the CLM4.5 and ORCHIDEE were not converted into the matrix forms, one plant C pool and a fixed CUE (i.e., $b1$) and k of it were used to represent plant C dynamics in the matrix forms. Plant CUE in the matrix-based CLM4.5 and ORCHIDEE were assigned as 0.35 and 0.5, respectively, the average values revealed in the versions participated in CMIP5 (Wei et al., 2022); k of the plant C pool was set empirically as 0.00004 $g\,g^{-1}\,day^{-1}$ in both models (Montané et al., 2017). Time constant bs were used in the original DALEC2 and CASA; these coefficients were directly used

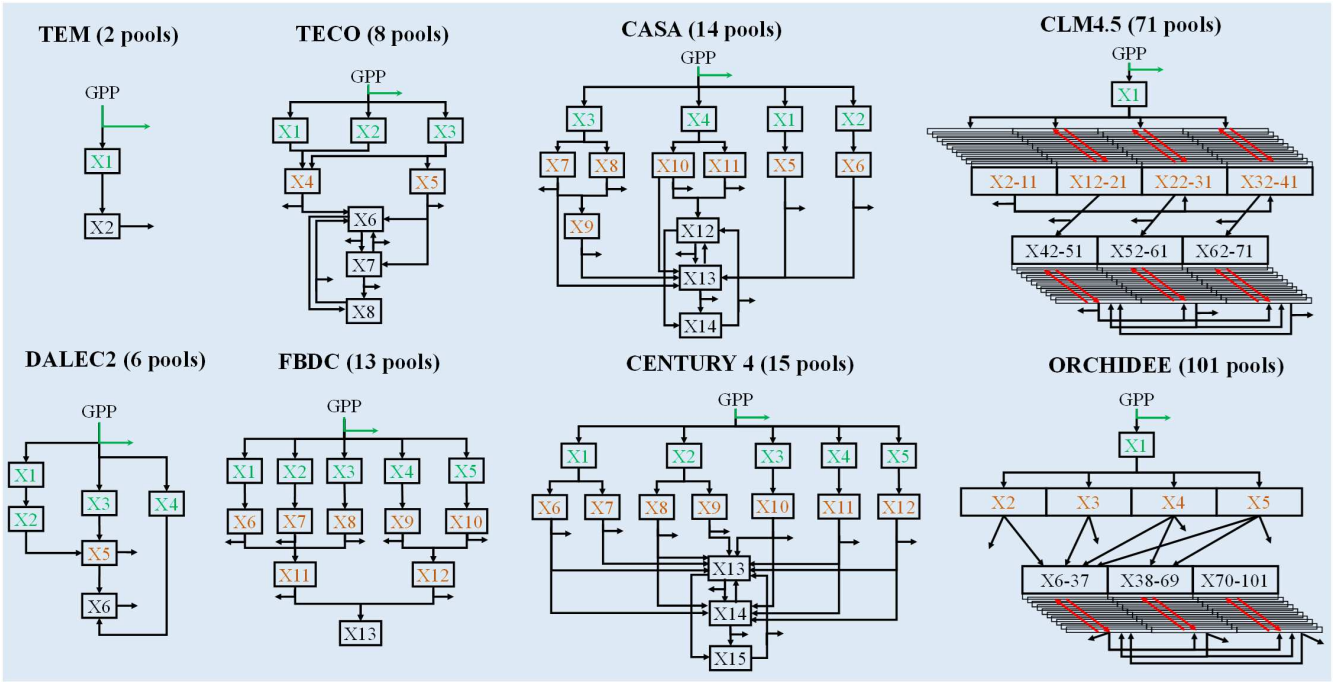

Unified matrix C model: $$\frac{dX(t)}{dt} = \beta(t)B \times u(t) - (A\xi(t)K + V) \times X(t)$$

FIGURE 1 Consolidating eight land C models into a unified matrix form. All models simulate land C cycle from gross primary production (GPP) to autotrophic respiration (blue arrow), heterotrophic respiration (black arrow), and plant (green box), litter (orange box, binned with soil in the TEM), and soil (black box) C pools. $X_{1, 2, 3, \ldots}$ indicates different C pools. In the CLM4.5 and ORCHIDEE, red arrow indicates vertical transfer process. In the unified matrix form, B indicates time-averaged coefficients of C allocation from GPP to different plant components, $\beta(t)$ indicates modifier of B at time t, $u(t)$ indicates GPP at time t, A indicates coefficients of transfer among C pools, ξ indicates environmental scalars, K indicates baseline turnover rate of C pools, V indicates vertical transfer coefficients, and $X(t)$ indicates C pool sizes at time t. Full names of the models can be seen in Table S1. [Colour figure can be viewed at wileyonlinelibrary.com]

in the matrix forms. The original FBDC and CENTURY4 adopted time constant coefficients of C allocations from NPP to plant tissues, without a simulation of GPP; a multiplication of these time constant coefficients by 0.5 (assumed plant CUE) were used as *b*s in the matrix forms.

Values of the other model parameters were directly extracted from the original models, though sometimes with modifications or simplifications. First, C transfers from the plant pools to litter pools in the original CLM4.5 and ORCHIDEE were simplified as the transfer of C from a single plant pool to multiple litter pools in the matrix forms; nevertheless, the proportions of C transfers from plant pool to litter pools are generally the same as in the original models. Such a simplification does not enable a comparison of C dynamics among models at plant tissue level, but should not affect C dynamics much at the ecosystem level. Second, the transfers of C from foliage and fine roots to structural and metabolic litters and further to soil are controlled by the lignin to N ratio in the plant materials in the CENTURY4; these transfer coefficients were parameterized based on a constant lignin to N ratio of black spruce. Coefficients of C transfer among pools are constant in the original TEM, DALEC2, TECO, FBDC, and CASA; these coefficients were extracted and directly used as *a*s in the matrix forms.

Third, *k* of each C pool was firstly extracted, or calculated based on soil particle size at the study site (for active soil C pool in the CENTURY4, CLM4.5, and ORCHIDEE only), from the original models, and then standardized with a reference temperature of 20°C, whenever it is temperature dependent. Fourth, ξ of each C pool was firstly calculated in the same way as in the original models, and then standardized with a reference temperature of 20°C (i.e., ξ_T at 20°C was set as 1), in correspondence to the standardization of *k*s by temperature. Note that different types of temperature measurements have been used to calculate ξ_T in these models, for example, using monthly mean air temperature in the TEM versus daily mean soil temperature in the CLM4.5 to calculate the ξ_T of soil C turnover. Therefore, even after our standardizations, temperature scalars could still differ among models under the same environmental conditions (e.g., soil temperature at 20°C). Moreover, it is a challenge to standardize water scalars across models to the same water conditions, because the water scalars of soil C pools were either not calculated (e.g., the FBDC) or calculated based on soil water content

(e.g., the TECO), soil matric potential (the CLM4.5), or potential evapotranspiration (the CENTURY4), though they ranged between ~0 and 1 in all models. Therefore, water scalars in the original models were used in the matrix models. Finally, *vs* in the matrix models were parameterized the same as in the original models, whenever vertical discretization is considered, that is, in the CLM4.5 and ORCHIDEE; for the other models that do not consider vertical discretization, all *vs* were set as 0.

2.3 | Model simulations and validations

To run the eight matrix models, we generated some of the required forcing data (i.e., GPP and soil temperature and water content of 0–100 cm depth at an interval of 10 cm) in each experimental treatment with a full version of the TECO model, which couples land C, water, and energy dynamics at an hourly time step (Huang et al., 2017; Ma et al., 2017). The model is driven by six climate variables, including precipitation, wind speed, solar radiation, air temperature, relative humidity, and vapor pressure deficit. Simulated GPP and a few other C variables (e.g., leaf C pool) were calibrated with their measurements in each treatment (Figure S1).

The above forcing data in each experimental treatment were used to drive all the eight models to simulate ecosystem C dynamics (soil in the top meter was considered). As a typical modeling practice on initial condition, the ecosystem was assumed to be in a steady state at the start of our simulation (i.e., the year 2011), as indicated by the measured NEP before the start of experiment ($0.082 \pm 0.101\,kg\,C\,m^{-2}\,year^{-1}$ during 2014–2015; Figure 2c). While this assumption may be a simplified one due to past land use change and transient CO_2 and climate effects, it enables us to model land C dynamics similarly to current ESMs, and thus provides a good comparison with ESM simulations. Under this assumption, initial C storage was set to be equal to the C storage in steady state in 2011 in each model. How this assumption would affect our traceability results were tested following. Spin-up of all models were performed with a semi-analytical solution (Xia et al., 2012).

Model simulations of NPP, NEP, and heterotrophic respiration were validated with their measurements in each experimental treatment during 2014–2018, which were reported by Hanson et al. (2020). Here we used measured NPP for validation, rather than for calibration, because comparing simulated NPP against its measurements enables an assessment of inter-model difference in plant CUE, which is known to be an important source of across-model spread in NEP. Pretreatment data were collected over multiple years prior to 2016 (i.e., 2011–2015), as summarized by Griffiths et al. (2017) and Hanson et al. (2020). The mean and standard deviation of NPP were calculated as a sum of the means and standard deviations, respectively, of the aboveground NPP of trees and shrubs, the NPP of *Sphagnum*, and the belowground NPP of trees, shrubs, and graminoids. Model simulations of ecosystem C storage were validated with its empirical estimate in 2012, which is a sum of plant C pool in Hanson et al. (2017) and top-meter soil C stock in Tfaily et al. (2014). Model performance in simulating the above C variables were assessed based on the root mean square error (RMSE).

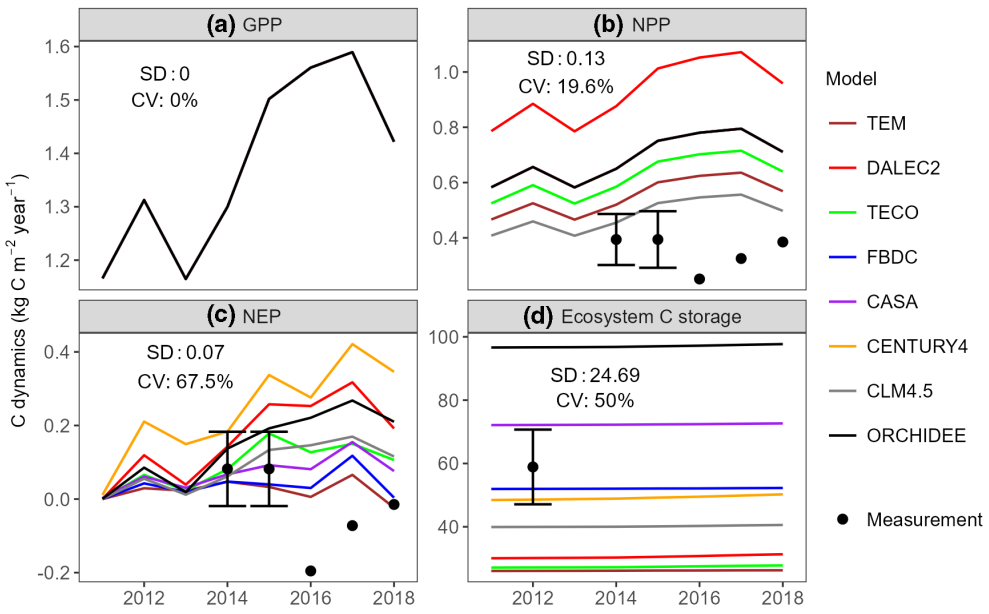

FIGURE 2 Simulated and measured ecosystem C dynamics in a northern peatland. Model simulated (a) gross primary production (GPP), (b) net primary production (NPP), (c) net ecosystem production (NEP), and (d) ecosystem C storage under the ambient condition; measurements are indicated by the black points, with the error bars indicates standard deviations. In each subplot, the standard deviation (SD) and coefficient of variance (CV) of time-averaged simulations are shown. [Colour figure can be viewed at wileyonlinelibrary.com]

2.4 | Analyses of model simulations

Reasons for across-model spreads in the ecosystem C dynamics were explored using a transient traceability analysis and a parameter manipulation analysis (Figure S2). Both analyses were performed on yearly simulations for demonstration, though all eight matrix models run daily or monthly. The transient traceability analysis was modified from Jiang et al. (2017) and J. Zhou et al. (2021), based on the mathematical foundation described by Luo et al. (2017). In brief, across-model spread in ecosystem C storage can be attributed to inter-model variation in C storage capacity (X_C, the maximum amount of C that an ecosystem can store) and C storage potential (X_P, the difference between X_C and ecosystem C storage). The variation in X_C was further traced to variations in NPP and ecosystem C residence time (τ_E). The variation in NPP was totally due to variation in plant CUE, given the same GPP for all models; the variation in τ_E was attributed to variations in baseline C residence time (τ_b) and ξ. The variation in ξ was attributed to variations in ξ_T, ξ_W, and ξ_O, which were further traced to the specific functions calculating these scalars in each model. Contributions of these diagnostic variables (e.g., X_C, X_P, and τ_E) to across-model spread in ecosystem C storage were quantified using a hierarchical partition method (Chevan & Sutherland, 1991) with the "hier.part" package version 1.0.6 in R version 4.1.3 (R Core Team, 2020).

To explore how the traceability results would be affected by our major model simplifications (i.e., using fixed GPP and time constant C allocation coefficients) and the steady state assumption, additional model runs were performed. Specifically, the impacts of model simplifications were examined by model runs with randomly scaled GPP and/or C allocation coefficients in each model, within the magnitudes of variations shown in the current generations of ESMs, that is, a 2.5-fold variation in GPP, and a plant CUE between 0.3 and 0.7 (Wei et al., 2022). For GPP scaling, the original GPP values in a model were multiplied by a random value between 0.57 and 1.43, to create a 2.5-fold (1.43/0.57 = 2.5) variation in GPP without a change in its mean (mean of random values between 0.57 and 1.43 would be approximately 1.00) across models. For the scaling of C allocation coefficients, the sum of *B* matrix in each model was set as a random value between 0.3 and 0.7, and $\beta(t)$ of each plant C pool in each model was multiplied by a random value between 0.6 and 1.4 to generate time-variable C allocation coefficients; 1.4 was used as the upper limit of the modifier of $\beta(t)$ to avoid a plant CUE over 1. Given the randomization processes, the above tests were repeated five times. The impacts of the steady state assumption were tested by two another model runs, in which initial C storage was set as half or twice of the C storage in the steady state for each C pool in each model.

For the parameter manipulation analysis, the eight matrix models were manipulated in five sequential steps to shrink their simulations, which were standardizing plant CUE, baseline C residence time, environmental scalar, and vertical transfer coefficients, and homogenizing decomposition coefficients. The manipulations were ordered based on the C flow order (Figure 1) as well as on our prior knowledge of their relative importance. First, plant CUE of all models were set to be their average (i.e., 0.484), by rescaling all *b*s (i.e., cells in the *B* matrix) in a model in the same proportion, in order to achieve the same NPP across models. Second, τ_b of all models were set to be their average (i.e., 52.77 years), by increasing or decreasing all *k*s in a model in the same proportion. Third, ξ of all models were set to be their average for plant and soil (including litter) C pools separately at each time step; this setting is based on the fact that ξ is always different between plant and soil C pools but not among multiple plant C pools or multiple soil C pools (Text S1). Fourth, *v*s of the vertically resolved models (i.e., CLM4.5 and ORCHIDEE) were set to be zero. Finally, *k* of all plant or soil (including litter) C pools in a model were set as their approximate averages across models (plant C pools: 0.0002 $g\,g^{-1}\,day^{-1}$; soil C pools: 0.00005 $g\,g^{-1}\,day^{-1}$), and then rescaled to achieve the standardized τ_b (i.e., 52.77 years) as in the Second step. To explore how the order of parameter manipulations would affect our results, alternative manipulation orders, for example, standardizing ξ before the standardization of τ_b, were also tested.

2.5 | Statistical analysis

Linear regression analysis was used to determine the effects of eCO_2 and warming as well as their interaction on both measured and simulated C fluxes, including GPP, NEP, NPP, and heterotrophic respiration. The eCO_2 was treated as a factor variable, with its effect on a C flux expressed as a percentage change in the eCO_2 treatments in comparison to the ambient CO_2 treatments. Warming level (i.e., ambient condition +0, 2.25, 4.5, 6.75, and 9.0°C, respectively) was treated as a numeric variable, with its effect on a C flux expressed as a change in the flux rate per °C warming. The regression analyses adopted data during the treatment period (i.e., 2016–2018) only, and were performed using the "lm" function in R version 4.1.3.

3 | RESULTS

3.1 | Ecosystem C dynamics under the ambient condition

There were divergent simulations of ecosystem C dynamics among models under the ambient condition (Figure 2). Simulated NPP varied from a time average of 0.48 $kg\,C\,m^{-2}\,year^{-1}$ in the CLM4.5 to 0.93 $kg\,C\,m^{-2}\,year^{-1}$ in the DLAEC2; these simulations were much higher than the measurements (0.25–0.39 $kg\,C\,m^{-2}\,year^{-1}$ during 2014–2018) (Figure 2b). Simulated NEP ranged between a time average of 0.02 and 0.24 $kg\,C\,m^{-2}\,year^{-1}$ across models (Figure 2c); models generally simulated NEP well in 2014 and 2015, but overestimated it after that, that is, simulations of −0.02 to 0.42 $kg\,C\,m^{-2}\,year^{-1}$ versus measurements of −0.20 to 0.01 $kg\,C\,m^{-2}\,year^{-1}$ during 2016–2018 (Figure 2c). Simulated ecosystem C storage varied 3.7 folds among models, though their average (49.4 $kg\,C\,m^{-2}$) was comparable to the

measurement (58.9 ± 11.8 kg C m^{-2}) (Figure 2d). The RMSE of NPP increased in the order of CLM4.5 < TEM < TECO < CASA = CENTURY4 = FBDC = ORCHIDEE < DALEC2, the RMSE of NEP in the order of TEM < CLM4.5 < ORCHIDEE < FBDC < CASA < TECO < DALEC2 > CENTURY4, and the RMSE of ecosystem C storage in the order of FBDC < CENTURY4 < CASA < CLM4.5 < DALEC2 < TECO < TEM < ORCHIDEE (Figure 2; Figure S3).

Traceability analysis showed that across-model spread in ecosystem C storage was attributed primarily to inter-model variation in X_C (82.2% of the variation), and a less degree to X_P (17.8%) (Figure 3a); the X_C (27.2–125.6 kg C m^{-2}) was, on average, five folds larger than the X_P (1.1–28.6 kg C m^{-2}) (Figure 3b,c). The variation in X_C was attributed primarily to inter-model variation in τ_E (75.9%) and much less to NPP (6.3%) (Figure 3a), which differed by factors of 4.3 (41.0–181.6 years) and 1.9 (0.48–0.93 kg C m^{-2} year^{-1}), respectively, among models (Figure 3d,e). Since GPP was the same for all models, variation in NPP was totally attributed to variation in plant CUE (Figure 3a). The variation in τ_E was attributed more to variation in τ_b (63.2%) than to variation in ξ (12.8%) (Figure 3a). The τ_b (16.2–110.0 years) and the ξ (0.28–0.82) differed by factors of 6.8 and 2.9, respectively, among models (Figure 3f,g). Although ξ_T increased with soil temperature in all models, the response curve differed largely among models (Figure S4a–h; Text S1). ξ_W increased with soil water content from 0.90 to 0.95 cm^3 cm^{-3} in the ORCHIDEE, but decreased slightly in the FBDC, without any gradual change in the other models (Figure S4i–p).

After GPP and plant CUE were rescaled according to variations revealed in the current generations of ESMs, they explained 7.3%–22.6% (mean 16.3%) and 6.6%–31.5% (17.7%), respectively, of inter-model variation in ecosystem C storage (Figure 4b; Figure S5), which were essentially higher than those shown in the default traceability analyses (0% and 6.3%, respectively) (Figure 4a). Correspondingly, the proportions explained by τ_b, ξ, and X_P decreased from 63.2% to 42.1%, from 12.8% to 8.5%, and from 17.8% to 15.4%, respectively (Figure 4a,b). The proportions estimated by the modified traceability analyses are generally comparable to those in a previous traceability analysis of global C simulations in the CMIP5 and CMIP6 (Figure 4). Tests of the steady state assumption showed that, after initial ecosystem C storage was set as half (or twice) of the value in the steady state in each model, the proportion explained by X_P increased from 17.8% to 42.2% (or 39.9%), and the proportions explained by other variables (e.g., X_C) correspondingly decreased (Table S2).

Sequentially manipulating model parameters shrunk model simulations (Figure 5). Standardizing plant CUE reduced inter-model variations in ecosystem C storage and cumulative NEP from 50.0% to 47.2% and from 67.5% to 62.6%, respectively, without an impact

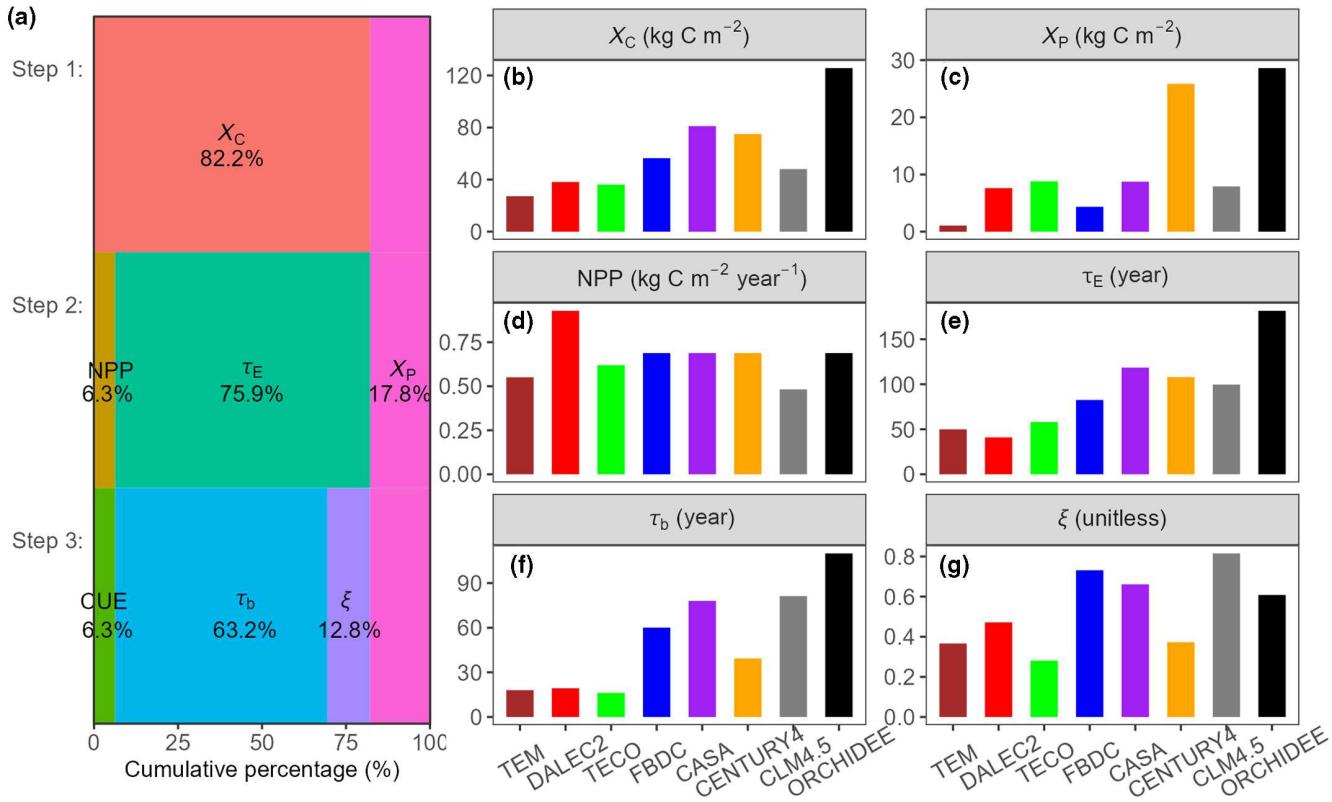

FIGURE 3 Transient traceability analysis of simulated ecosystem C dynamics. (a) Across-model spread in ecosystem C storage is traced into model components by three steps. First, the spread is attributed to inter-model variations in (b) C storage capacity (X_C) and (c) C storage potential (X_P). Second, the variation in X_C is attributed to inter-model variations in (d) net primary production (NPP) and (e) ecosystem C residence time (τ_E). Third, the variation in τ is attributed to inter-model variations in (f) baseline C residence time (τ_b) and (g) environmental scalars (ξ); the variation in NPP is attributed wholly to inter-model variation in plant C use efficiency (CUE). [Colour figure can be viewed at wileyonlinelibrary.com]

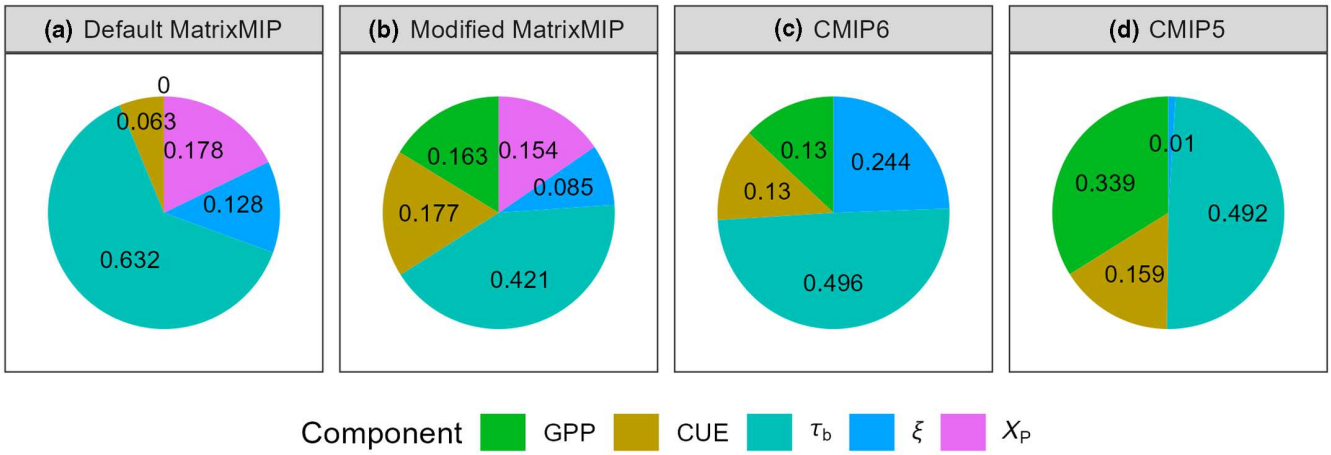

FIGURE 4 Comparison of traceability results among model intercomparison projects (MIPs). Traceability results in our (a) default Matrix-based MIP (Default MatrixMIP), (b) MatrixMIP with more complete consideration of inter-model variations in gross primary production (GPP) and C allocation coefficients (Modified MatrixMIP), and the phases (c) 6 and (d) 5 of the Coupled Model Intercomparison Project (CMIP6 and CMIP5, respectively). Model components include GPP, plant C use efficiency (CUE), baseline C residence time (τ_b), environmental scalar (ξ), and C storage potential (X_P). In (a), the default MatrixMIP used the same GPP to drive all models, therefore the contribution of GPP is 0. Results in (c) and (d) are redrawn from Wei et al. (2022), which cannot attribute across-model spread to X_P. [Colour figure can be viewed at wileyonlinelibrary.com]

on τ_E (Figure 5a–f). Thereafter, standardizing τ_b reduced variations in the C storage and τ_E from 47.2% to 37.0% and from 49.5% to 39.5%, respectively, and also reduced variation in the NEP slightly from 62.6% to 61.9% (Figure 5d–i). Alternatively, if ξ, instead of τ_b, was standardized in the second step, variations in the C storage and τ_E would increase, instead of decrease, from 47.2% to 66.2% and from 49.5% 66.5%, respectively, and the variation in NEP would decrease from 62.6% to 22.5% (Figure S6). Comparison of results between the two different orders showed a larger contribution of τ_b than ξ to the variation in ecosystem C storage while an opposite rank of contributions to the variation in NEP. Standardizing ξ after the standardization of τ_b reduced variations in the NEP, C storage, and τ_E from 61.9% to 12.2%, 37.0% to 0.1%, and from 39.3% to 0.1%, respectively (Figure 5g–l). Standardizing *vs* in the fourth step had minor influences on the variations in C storage, NEP, and τ_E (Figure 5j–o). Homogenizing *ks* in the fifth step reduced variation in the NEP from 12.2% to 0.1% (Figure 5n,q). After the above five manipulations, the remaining minor variations in C storage, NEP, and τ_E (all ≤ 0.1%; Figure 5p–r) were due to the different time steps (i.e., daily vs. monthly) used by the models.

3.2 | Responses of ecosystem C dynamics to experimental treatments

In general, both measured and simulated NEP responded negatively to warming, with measured response of −0.026 kg C m^{-2} $year^{-1}$°C^{-1} and simulated responses of −0.061 to 0.001 (mean − 0.023) kg C m^{-2} $year^{-1}$°C^{-1} (Figures 6k–t and 7d). The simulated responses became more divergent among models with warming (Figure 6k–t). The negative responses were mainly because of the positive responses of heterotrophic respiration to warming in both the measurements (0.016 kg C m^{-2} $year^{-1}$°C^{-1}) and the simulations (0–0.062 kg C m^{-2} $year^{-1}$°C^{-1}), since NPP responded minorly to warming (Figure 7d–f). The positive warming responses of heterotrophic respiration in models were attributed to the increases in ξ_T with warming (Figure S4a–h), since τ_b did not respond to warming in any model (Figure 8f). RMSE of the NEP, but not that of the NPP or heterotrophic respiration, increased under warming (Figure S3).

Measured NEP responded minorly (3.2%) to eCO_2 (Figures 6a–j and 7a). Simulated NEP also responded minorly to eCO_2 in the CLM4.5 (−0.9%) and ORCHIDEE (−2.4%), but positively (26.9%–52.4%) in the other models (Figure 7a). The positive simulated responses were related to the increases in X_P and X_C under eCO_2 (Figure 8; Figure S7). The increase in X_C was attributed to the increases in simulated NPP (34.8%–67.1%) and GPP (62.4%) under eCO_2 (Figure 8c,e); however, neither the measured NPP nor the measured GPP responded significantly to eCO_2 (Figure 7b; Figure S8). Minor responses of NEP to eCO_2 in the CLM4.5 and ORCHIDEE were due to their relatively high τ_Es, and thus relatively slow responses to eCO_2, than the other models (Figure 8d). RMSE of both the NPP and the NEP increased under eCO_2 (Figure S3).

4 | DISCUSSION

Many studies have compared land C simulations among models to understand the across-model spread in steady states (e.g., Rafique et al., 2016; Todd-Brown et al., 2013; Wei et al., 2022). Some studies have also analytically analyzed the uncertainty of transient ecosystem C dynamics simulated by a single model after converting it into a matrix form (Jiang et al., 2017; Luo et al., 2017). Nevertheless, no study has analytically compared transient ecosystem C simulations under global change among multiple models.

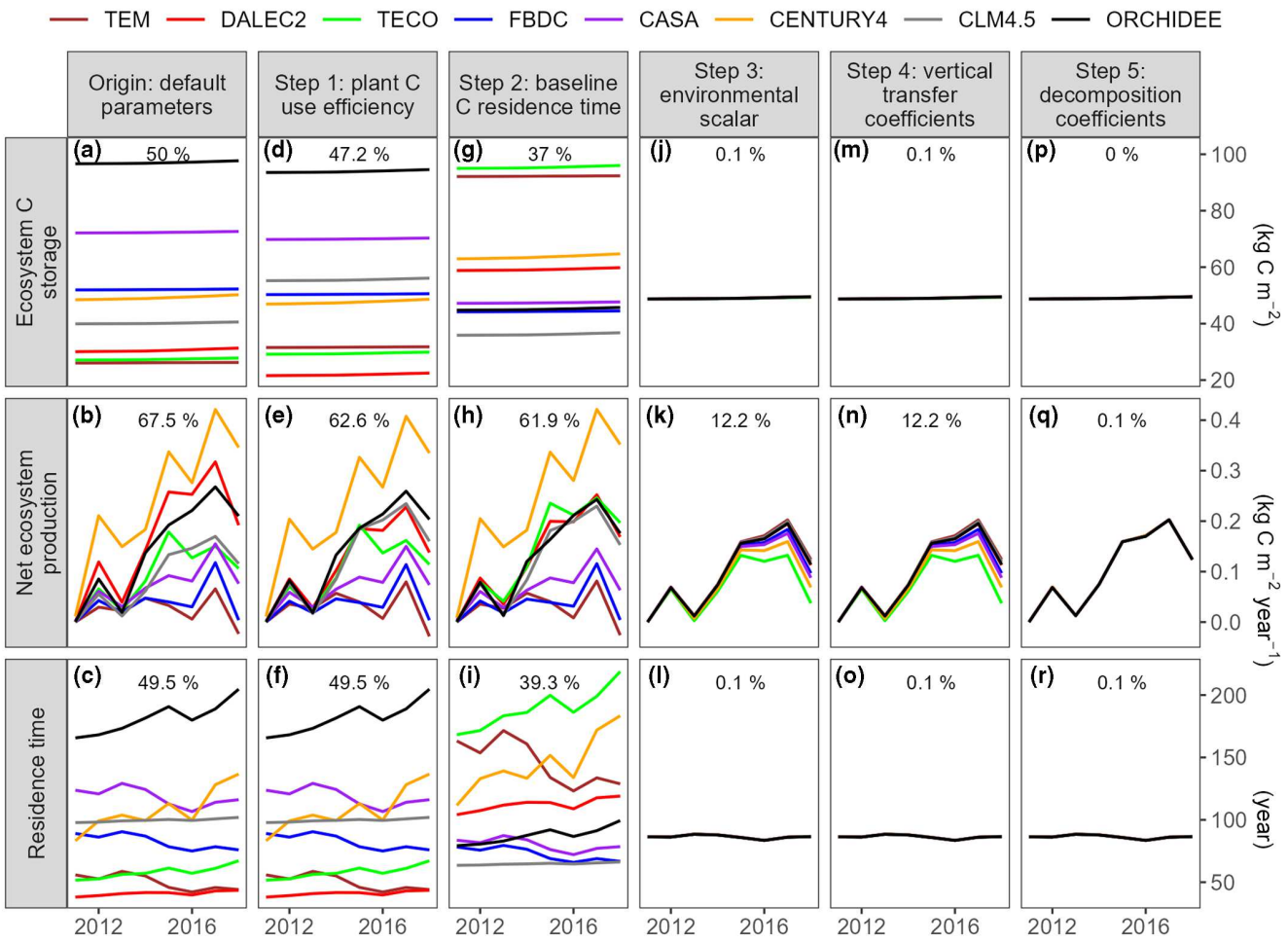

FIGURE 5 Across-model spread in ecosystem C dynamics are shrinkage after standardizing parameter values. Simulated ecosystem C storage, net ecosystem production, and C residence time in the (a–c) original model run and (d–r) model runs after Steps 1–5, respectively. Origin model run indicates model simulations with the default parameter values. Steps 1–5 indicate model simulations after sequentially standardizing plant C use efficiency, baseline C residence time, environmental scalar, and vertical transfer coefficients, and homogenizing decomposition coefficients. Percentage in each subpanel indicates the coefficient of variance of time-averaged simulations. [Colour figure can be viewed at wileyonlinelibrary.com]

By converting the C cycle modules of eight land models into a unified matrix form, our study analytically traced the across-model spread in simulated transient C dynamics under global change to its sources in the SPRUCE experiment. Since the matrix models ran in standalone, some model simplifications were made during the model conversion, mainly of using fixed GPP and time constant C allocation coefficients (Text S1). Therefore, we cannot consider uncertainty in GPP caused by feedbacks to it from downstream processes (e.g., C allocations to plant tissues) or variables (e.g., nutrient availability) in some models (e.g., the CLM4.5), and could also not fully consider model differences in C allocation coefficients. Nevertheless, how these simplifications may affect our results have been explored by model runs with randomized GPP and C allocation coefficients in the ranges revealed by the current generations of ESMs. Moreover, how the assumption of steady state at the start of model simulation may affect our traceability results has been explored by model runs with non-steady state initial C storages. These tests suggest that our default model comparison may underestimate the relative contributions of GPP, C allocation coefficients, and X_P to the across-model spread in ecosystem C dynamics. Nevertheless, all the tests showed that τ_b contributed the most to the across-model spread in ecosystem C storage (Figure 4; Figure S5; Table S2). This conclusion was also supported by our parameter manipulation analyses (Figure 5; Figure S6).

Our parameter manipulation analysis clearly demonstrated the major contribution of ξ to the spread. Models generally captured the negative response of NEP to warming, but differed largely in the magnitude of response. The difference was traced to the varied τ_b and temperature sensitivity of ξ_T among models. While there was a lack of response of NEP to eCO_2 in the measurement, simulated NEP responded positively to eCO_2 in most models. The positive responses in models were attributed to the modelled positive responses of NPP to eCO_2. Our matrix-based approach not only analytically traced the across-model spread in ecosystem C storage to its sources as done in previous studies (Jiang et al., 2017; Rafique et al., 2016; Wei et al., 2022), but also analytically traced spreads in NEP and its responses to global change manipulations to their sources, which has not been achieved previously.

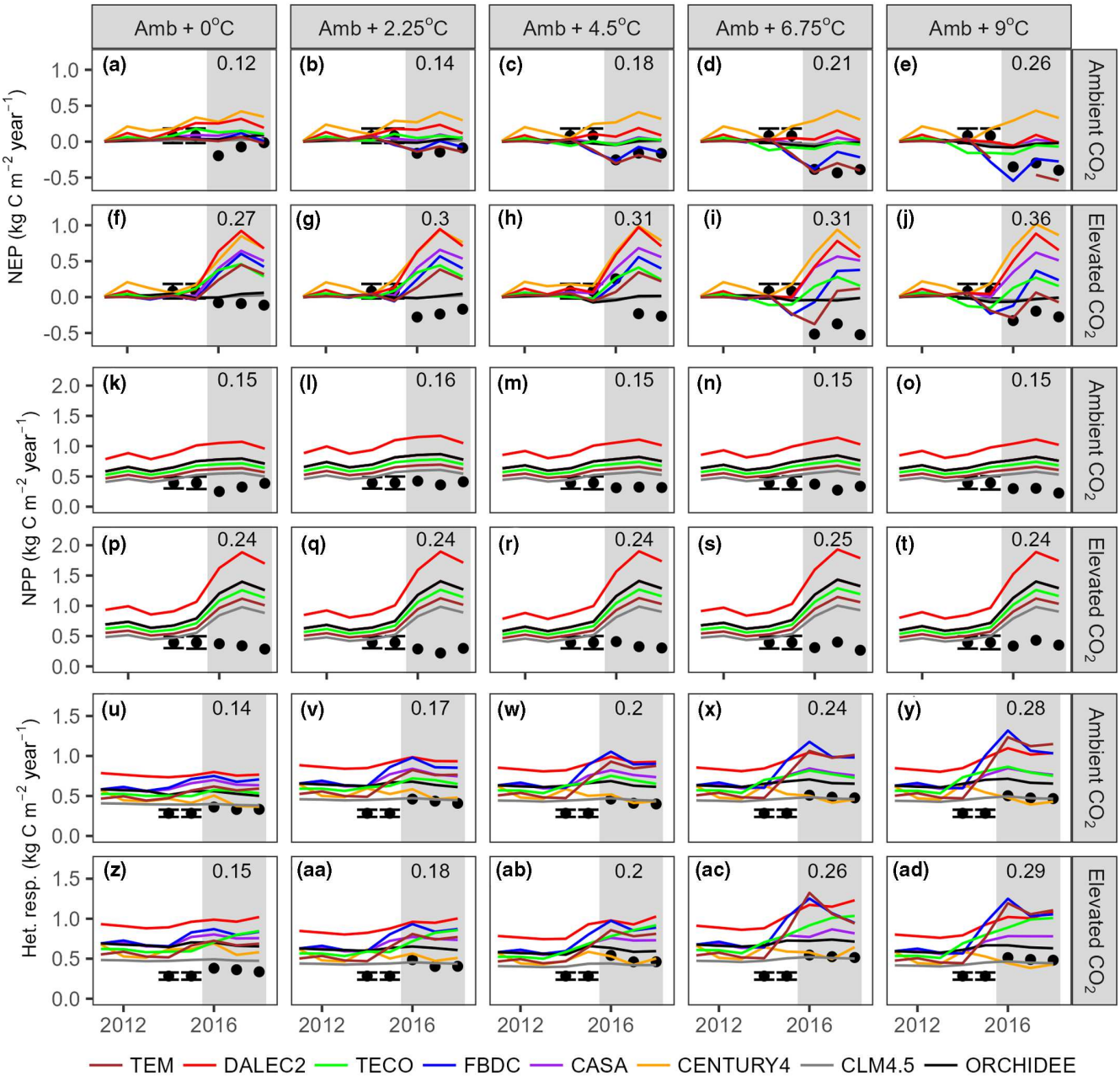

FIGURE 6 Comparison between simulated and measured C fluxes in different experimental treatments. Carbon fluxes include yearly (a–j) net primary production (NPP), (k–t) net ecosystem production (NEP), and (u–ad) heterotrophic respiration (Het. resp.). Experimental treatments include a factorial combination of five warming levels (i.e., ambient +0, 2.25, 4.5, 6.75, and 9.0°C) and two atmospheric CO_2 levels (i.e., ambient and elevated CO_2). Simulations are indicated by color lines (colors indicate models); the means and standard deviations of measurements are indicated by black points and error bars, respectively. In each subplot, the shaded area indicates the treatment period (i.e., during 2016–2018), and the number in it indicates the standard deviation of time-averaged simulations during the period. [Colour figure can be viewed at wileyonlinelibrary.com]

4.1 | Ecosystem C dynamics under the ambient condition

All models generally overestimated NEP, which was mainly due to the overestimation of NPP. NPP is a multiplication of GPP and plant CUE. Since GPP is validated by only a few days of measurements, we cannot rule out the possibility that yearly GPP is overestimated here; however, plant CUE was more likely to be overestimated. Plant CUE was simply assigned as 0.5 in models that start C simulations from NPP rather than GPP, that is, the FBDC, CENTURY4, and CASA (Text S1). Although this value is only slightly higher than the global average of observations (0.45), observed plant CUE varies largely among sites and suffer from a large uncertainty as well (Wei et al., 2022; Zhang et al., 2014). The overestimation of NPP, in combination with the comparable ecosystem C storage between the model average and the measurement

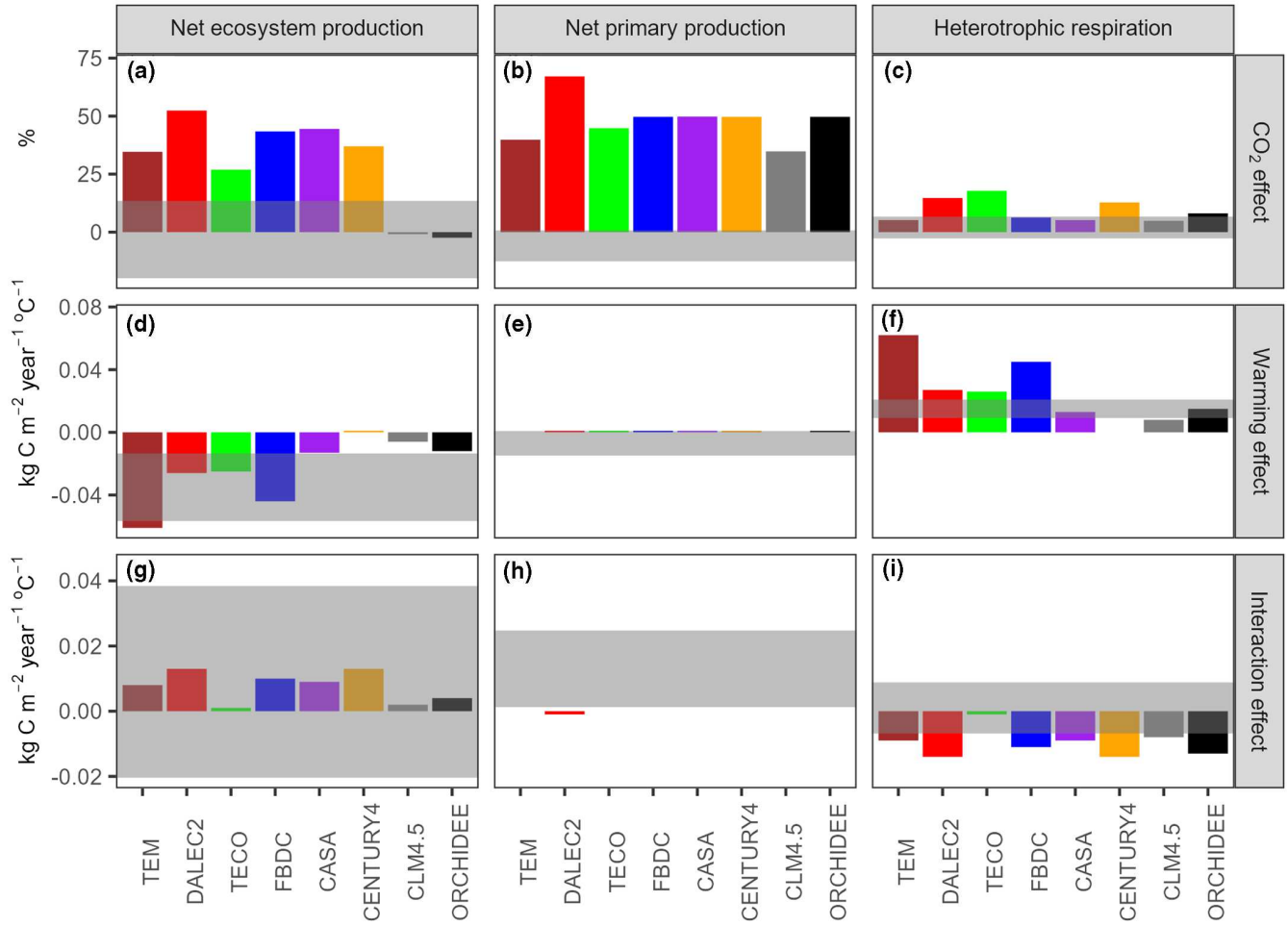

FIGURE 7 Comparison between simulated and measured treatment effects on ecosystem C dynamics. Effects of elevated CO_2, warming and their interaction on net ecosystem production (a, d, and g, respectively), net primary production (b, e, and h, respectively), and heterotrophic respiration (c, f, and i, respectively) are compared between model simulations (bars) and measurements (shaded area, which indicates the 95% confidence interval). CO_2 effect is expressed as a percentage change in C flux rate under the elevated CO_2 concentrations in comparison to under the ambient CO_2 concentrations; warming effect and its interaction with CO_2 effect are expressed as an absolute change in C flux rate per °C warming. [Colour figure can be viewed at wileyonlinelibrary.com]

(Figure 2b,d), suggests that models generally underestimated τ_E. Indeed, heterotrophic respiration, which indicates soil C turnover rate, was overestimated by models across experimental treatments, though with a less extent in the vertically resolved models (i.e., the CLM4.5 and ORCHIDEE models) than in the vertically unresolved ones (Figure 6u–ad). These findings are in line with the findings in recent global data-model comparisons (Shi et al., 2020; Wei et al., 2022), in which land τ_E is globally underestimated by models, especially over the northern high latitudes, and even by the vertically resolved models.

In general, across-model spread in ecosystem C dynamics can be attributed to inter-model variations in C input, τ_E, and internal C cycling processes such as C transfers among pools. Although such attributions cannot be fully explored here, our traceability analyses with considerations of uncertainties in GPP and C allocation coefficients showed that, τ_E was the major contributor to across-model spread in C storage. This result is in line with that in Wei et al. (2022), in which inter-model variation in τ_E contributed to 66.1% and 77.9% of the inter-model variation in land C storage in the CMIP5 and CMIP6, respectively. The increase in relative contribution of τ_E from CMIP5 to CMIP6 highlights the growing need for improved understanding of inter-model variation in land τ_E.

Inter-model variation in τ_E can be attributed to variations in τ_b and ξ. Similar as revealed by traceability analyses of CMIP5 and CMIP6 simulations (Wei et al., 2022), our traceability analysis attributed variation in τ_E more to τ_b than to ξ (Figure 4). A similar trend but a smaller difference between the two components was revealed by our parameter manipulation analysis (Figure 5; Figure S6). This difference among analyses was because that, the statistical method used in the traceability analysis (i.e., hierarchical analysis) cannot accurately attribute variation in τ_E to its two components that are positively correlated ($r = .76$, $p = .28$, $n = 8$). Given such a positive correlation, standardizing ξ before the standardization of τ_b even increased inter-model variation in ecosystem C storage (Figure S6). Moreover, inter-model variation in NEP was attributed more to variation in ξ than to variation in τ_b (Figure 5; Figure S6), and increasing across-model spread in NEP

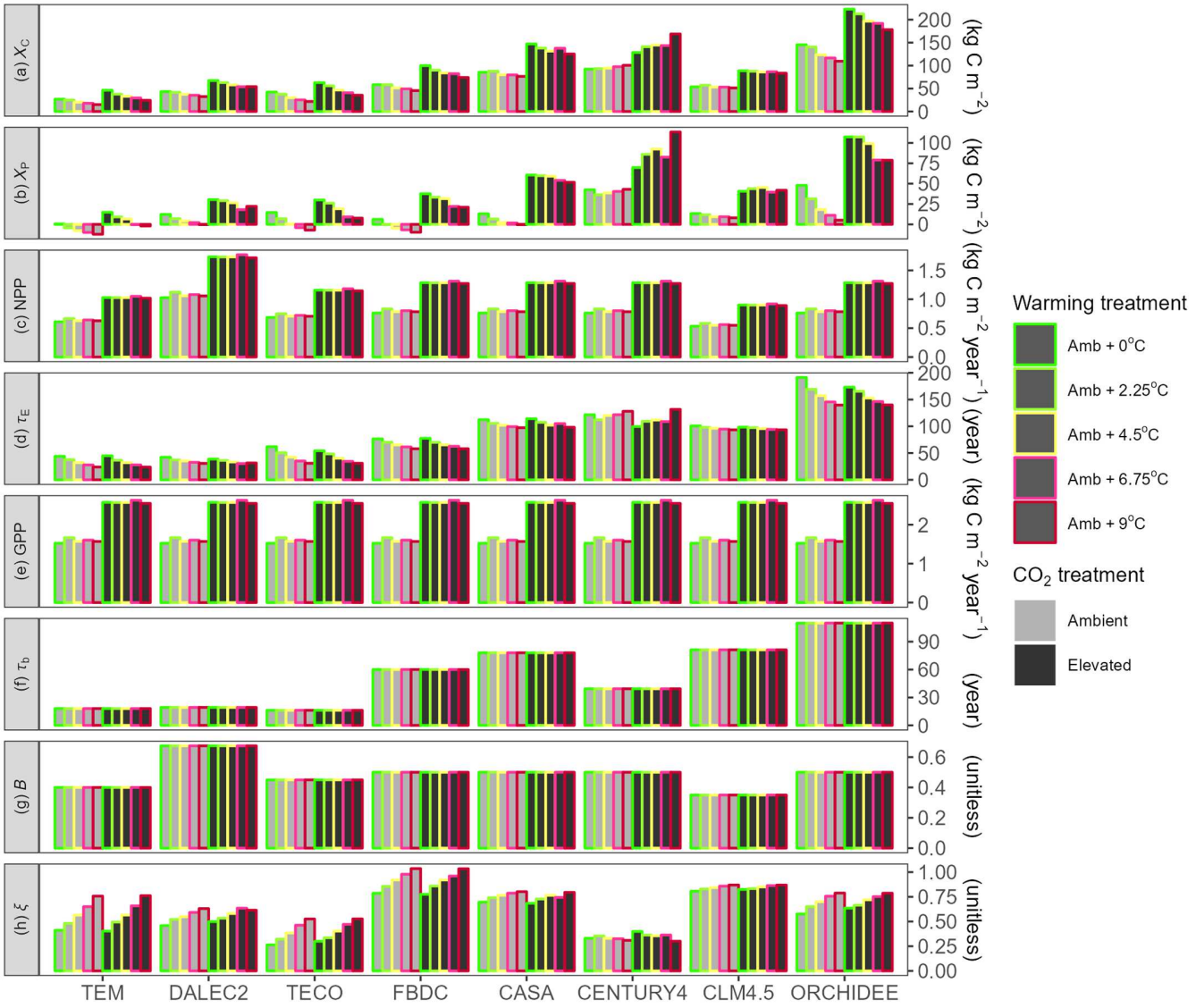

FIGURE 8 Traceable model components under different experimental treatments. Comparisons of (a) C storage capacity (X_C), (b) C storage potential (X_P), (c) net primary production (NPP), (d) ecosystem C residence time (τ_E), (e) gross primary production (GPP), (f) baseline C residence time (τ_b), (g) C allocation coefficients (B), and (h) environmental scalar (ξ) among models in a factorial combination of five warming levels (ambient condition +0, 2.25, 4.5, 6.75, and 9.0°C, respectively) and two CO_2 concentration levels (ambient CO_2, and elevated CO_2 up to 900 ppm, respectively). [Colour figure can be viewed at wileyonlinelibrary.com]

with warming was attributed to the increase in inter-model variation in ξ (Figures 6a–j and 8h). These findings highlight the underappreciated contribution of ξ to across-model spread in transient C dynamics. The findings also reflect the fact that, ξs in models are calculated using distinct functions of C turnover responses to environmental changes (e.g., exponential, unimodal, and logistic functions) and different environmental variables (e.g., monthly mean air temperature in the TEM vs. daily mean soil temperature in the CLM4.5 for soil C pools) (Text S1). These functions were primarily developed based on limited and short-term empirical data, obtained using diverse methods (e.g., laboratory or field measurements of soil respiration and isotopic tracer) from individual sites (Burke et al., 2003).

To improve model performance in simulating ecosystem C dynamics, an increasing number of C pools have been created in models to represent more biogeochemical processes (Bonan & Doney, 2018; Koven et al., 2013; Luo & Schuur, 2020). Our results showed that model structure (i.e., the number of C pools and C transfers among the pools) contributed much less to the across-model spreads in C storage and NEP than model parameters (Figure 5). This result was probably because that the turnover of C pools in all models are generally based on the same (i.e., first-order) kinetics. Although the complex models (i.e., the CLM4.5 and ORCHIDEE) captured the lack of NEP response to eCO_2, they failed to predict the lack of NPP response of eCO_2 (Figure 7). The lack of NEP response was likely attributed to the lack of NPP response in the measurements, but was probably associated with the relatively high τ_bs, which indicate the relatively slow responses to global change and disturbances, in the two complex models, compared to the simpler ones (Figure 8f). These

results suggest that the two complex models captured the pattern of NEP response to eCO_2 due to an incorrect reason. Moreover, the underestimated temperature sensitivity of NEP in the two complex models was probably associated with their relatively high τ_bs and relatively low temperature sensitivity of ξ in comparison to the simpler ones (Figures 7d and 8). Overall, the complex models had similar performances with the simpler ones in simulating C dynamics at the ecosystem level. We propose that while more pools and processes can represent C cycle more in details, improved mechanistic representation of C cycling processes and parameterization are more essential to improve model performance at the ecosystem level.

4.2 | Ecosystem dynamics under elevated atmospheric CO_2 and temperature

Similar as the ELM-SPRUCE model in Hanson et al. (2020), our models generally captured the response of C fluxes (i.e., NEP, NPP, and heterotrophic respiration) to warming but failed to predict the general lack of response to eCO_2 at the SPRUCE site. This finding suggests that the current generation of land C models perform generally similar in capturing the nature of land C responses to global change. Measured NEP responded negatively to warming, but not responded to eCO_2 or its interaction with warming. These responses were mainly attributed to the corresponding responses of heterotrophic respiration: positive response to warming but no response to eCO_2 or its interaction with warming.

Although models generally captured the positive response of heterotrophic respiration to warming, there was a large inter-model difference in the magnitude of response to warming, that is, warming sensitivity. Our traceability analysis showed that this difference was attributed to inter-model differences in τ_b and/or the warming sensitivity of ξ_T (usually indicated by Q_{10}). For example, warming sensitivity of heterotrophic respiration was highest in the TEM (Figure 7d) due to its lowest τ_b among models (Figure 8f). Warming sensitivity of heterotrophic respiration is lowest in the CENTURY4 (Figure 7d), due to its low temperature sensitivity of ξ_T (Figure 8h). Since neither τ_b nor Q_{10} was measured at the site, we cannot distinguish which parameter(s) were biased in each model. Measurements of these parameters are highly needed to constrain model simulations of decomposition response to warming. While Q_{10} is relatively easy to be determined, determining τ_b of a soil is usually difficult. τ_b may be empirically determined by approaches such as stable isotope techniques (Bernoux et al., 1998) and long-term (>10 years) monitoring of soil organic C storage (Smith et al., 2020), or estimated by combining measurements such as ^{14}C signature of soil organic matter with data-model fusion techniques (e.g., data assimilation; López-Blanco et al., 2019; Luo et al., 2016; Luo & Schuur, 2020; Shi et al., 2020).

The response of NEP to eCO_2 was overestimated by all models, due to the overestimation of NPP response, which was at least partly further attributed to the overestimation of GPP response. Leaf-level response to eCO_2 in the woody plants at the SPRUCE site was evident as increased nonstructural carbohydrates and differential biochemical acclimation; nevertheless, community-level NPP gain in response to eCO_2 has yet to develop (Hanson et al., 2020). The lack of response in measurement has been attributed to the nutrient-limited conditions (mainly N-limited) at the site, which is expected to be eliminated with enhanced decomposition under warmer conditions (Hanson et al., 2020). Nutrients may affect NPP by multiple pathways, such as limiting photosynthesis rate (Liang et al., 2020), reducing plant CUE by increasing C allocation to nutrient acquisition and use (Manzoni et al., 2018), and altering the allocation of GPP to different plant tissues (Hartmann et al., 2020).

All models in this study did not consider nutrient impacts on C dynamics, though some of the original models (e.g., CLM4.5 and ORCHIDEE) did (Text S1). Nevertheless, the ELM-SPRUCE model also failed to predict the lack of response of NEP to eCO_2 at the site, though it includes a detailed treatment of N and P cycle dynamics and C–N–P interactions such as complex interactions between plants, microbes, and soils on soil N and P availability, and is validated by measurements such as measured N and P deposition rates and N and P concentrations of plants and fresh litter (Hanson et al., 2020). In fact, the responses of peatland C dynamics to eCO_2 remain poorly known, with mixed responses (e.g., positive response and lack of response) reported in previous studies (Fenner et al., 2007; Girardin et al., 2016). To improve our predictive understanding of peatland C responses to eCO_2 concentrations, multiple efforts are still needed, such as improved understanding of nutrient impacts on photosynthesis rate and C allocations, more realistic model representation of these impacts, and more observations to validate the new representations.

Predicting peatland C dynamics under global change remains a big challenge (Chaudhary et al., 2020; Wei et al., 2022). In this study, we have little empirical information on the model parameters, therefore in our parameter manipulation practice parameters were standardized to their averages across models for a demonstration purpose, instead of standardized to empirical values to constrain model predictions. Our comparisons between the measured and simulated C fluxes can shed lights on, but not constrain, the model parameters. Nevertheless, our study showed that the matrix approach of modeling enables an analytical understanding of across-model spread in C dynamics in a northern peatland under different global change treatments. Previous studies suggest that the matrix approach also facilitates a semi-analytical model spin-up (Xia et al., 2013), a sensitivity analysis of model parameters (Huang, Zhu, et al., 2018), and the assimilation of multiple data sources into complex land surface models (e.g., CLM4.5) (Tao et al., 2020), to understand and reduce uncertainties in model parameters and predictions (Luo et al., 2022). Beside C cycle modules or models, N and P cycle modules or models can also be consolidated in a matrix form (Hou et al., 2019; Lu et al., 2020). Therefore, we advocate efforts to implement matrix approach to biogeochemistry modules of the current generation of ESMs, ideally without any simplification in model structure or parameter, to perform inter-model comparisons and model-data comparisons, which will finally help understand model uncertainty and thereafter improve model performance.

5 | CONCLUSION

This study pinned down sources of the across-model spread in predicting ecosystem C dynamics in a global change experiment in a northern peatland. We first consolidated eight land C models into a unified matrix form, and then traced the across-model spread to its sources, according to the terms of the matrix equations. We found that the across-model spread in predicting C storage in the peatland was primarily due to inter-model variation in C residence time, which was further attributed mainly to the inter-model variation in baseline C residence time. The across-model spread in predicting NEP was mainly due to the inter-model variation in environmental scalars, and were shrunk to almost none after each of the model components were standardized. The eight models can generally capture the negative responses of NEP to warming, but differed largely in the magnitude of responses, due to varied baseline C residence time and temperature sensitivity of decomposition among models. Most models failed to predict a lack of responses of NEP to eCO_2 concentrations, due to the predicted CO_2 stimulation of NPP. Pinning down the sources of the across-model spreads in ecosystem C dynamics provides a scientific basis for developing more realistic models and gaining more reliable predictions. Although our study was performed in a peatland ecosystem with simplified matrix models, our matrix-based approaches provide a powerful way to understand causes of the across-model spreads both analytically and systematically, and thus offer pointers for effective improvement in predicting land C dynamics under global change with ESMs.

AUTHOR CONTRIBUTIONS

Yiqi Luo and Enqing Hou conceptualized and designed this study; Shuang Ma provided forcing data for the matrix models; Enqing Hou, Yuanyuan Huang, Yu Zhou, Hyung-Sub Kim, and Efrén López-Blanco converted models into the unified matrix form and ran model simulations; Enqing Hou and Yiqi Luo analyzed data; Enqing Hou wrote first draft; all authors contributed to writing and revisions.

ACKNOWLEDGMENTS

The authors thank Ning Wei for discussion on the work, and Professor Nigel Roulet and two anonymous reviewers for their constructive comments on this manuscript. This study was supported by the National Natural Science Foundation of China (32271644, 31870464), Guangdong Basic and Applied Basic Research Foundation (2022B1515020014), National Science Foundation Grant DEB (1655499; 2017884), US Department of Energy (DOE), Terrestrial Ecosystem Sciences Grant (DE-SC0020227), and the subcontract 4000158404 from Oak Ridge National Laboratory (ORNL) to Northern Arizona University. ORNL's work was supported by DOE, Office of Science, Office of Biological and Environmental Research. ORNL is managed by UT-Battelle, LLC, for DOE under contract DE-AC05-00OR22725. Hyung-Sub Kim was supported by the National Research Foundation of Korea (NRF-2018R1A2B6001012). Efrén López-Blanco and Mathew Williams thank Luke Smallman for support in calibrating the DALEC2 model for the site. Efrén López-Blanco has received funding from GreenFeedBack (Greenhouse gas fluxes and earth system feedbacks) funded by the European Union's HORIZON research and innovation program under grant agreement No 101056921. Part of this research was carried out at the Jet Propulsion Laboratory, California Institute of Technology, under a contract with the National Aeronautics and Space Administration.

CONFLICT OF INTEREST STATEMENT

The authors declare no competing interests.

DATA AVAILABILITY STATEMENT

All data and code used to generate this manuscript has been deposited at Figshare (https://doi.org/10.6084/m9.figshare.19918879.v1).

ORCID

Enqing Hou https://orcid.org/0000-0003-4864-2347
Yu Zhou https://orcid.org/0000-0002-5544-8342
Jianyang Xia https://orcid.org/0000-0001-5923-6665
Feng Tao https://orcid.org/0000-0001-6105-860X
Christopher Williams https://orcid.org/0000-0002-5047-0639
Daniel Ricciuto https://orcid.org/0000-0002-3668-3021
Paul J. Hanson https://orcid.org/0000-0001-7293-3561
Yiqi Luo https://orcid.org/0000-0002-4556-0218

REFERENCES

Bernoux, M., Cerri, C. C., Neill, C., & de Moraes, J. F. L. (1998). The use of stable carbon isotopes for estimating soil organic matter turnover rates. *Geoderma*, *82*, 43–58.

Bloom, A., & Williams, M. (2015). Constraining ecosystem carbon dynamics in a data-limited world: Integrating ecological "common sense" in a model–data fusion framework. *Biogeosciences*, *12*, 1299–1315.

Bonan, G. B., & Doney, S. C. (2018). Climate, ecosystems, and planetary futures: The challenge to predict life in Earth system models. *Science*, *359*, eaam8328.

Bradford, M. A., Wieder, W. R., Bonan, G. B., Fierer, N., Raymond, P. A., & Crowther, T. W. (2016). Managing uncertainty in soil carbon feedbacks to climate change. *Nature Climate Change*, *6*, 751–758.

Bridgham, S. D., Pastor, J., Dewey, B., Weltzin, J. F., & Updegraff, K. (2008). Rapid carbon response of peatlands to climate change. *Ecology*, *89*, 3041–3048.

Burke, I. C., Kaye, J. P., Bird, S. P., Hall, S. A., McCulley, R. L., & Sommerville, G. L. (2003). Evaluating and testing models of terrestrial biogeochemistry: The role of temperature in controlling decomposition. In C. D. Canham, J. J. Cole, & W. K. Lauenroth (Eds.), *Models in ecosystem science* (pp. 225–253). Princeton University Press.

Chaudhary, N., Westermann, S., Lamba, S., Shurpali, N., Sannel, A. B. K., Schurgers, G., Miller, P. A., & Smith, B. (2020). Modelling past and future peatland carbon dynamics across the pan-Arctic. *Global Change Biology*, *26*, 4119–4133.

Chevan, A., & Sutherland, M. (1991). Hierarchical partitioning. *American Statistician*, *45*, 90–96.

Ciais, P., Sabine, C., Bala, G., Bopp, L., Brovkin, V., Canadell, J., Chhabra, A., DeFries, R., Galloway, J., Heimann, M., Jones, C., Le Quéré, C., Myneni, R. B., Piao, S., & Thornton, P. (2013). Carbon and other biogeochemical cycles. In T. F. Stocker, D. Qin, G.-K. Plattner, M. Tignor, S. K. Allen, J. Boschung, A. Nauels, Y. Xia, V. Bex, & P. M. Midgley (Eds.), *Climate change 2013: The physical science basis. Contribution of Working Group I to the Fifth Assessment Report of the Intergovernmental Panel on Climate Change* (pp. 465–570). Cambridge University Press.

Collier, N., Hoffman, F. M., Lawrence, D. M., Keppel-Aleks, G., Koven, C. D., Riley, W. J., Mu, M., & Randerson, J. T. (2018). The International Land Model Benchmarking (ILAMB) system: Design, theory, and implementation. *Journal of Advances in Modeling Earth Systems*, *10*, 2731–2754.

Fenner, N., Ostle, N. J., McNamara, N., Sparks, T., Harmens, H., Reynolds, B., & Freeman, C. (2007). Elevated CO_2 effects on peatland plant community carbon dynamics and DOC production. *Ecosystems*, *10*, 635–647.

Friedlingstein, P., Cox, P., Betts, R., Bopp, L., Von Bloh, W., Brovkin, V., Cadule, P., Doney, S., Eby, M., Fung, I., Bala, G., John, J., Jones, C., Joos, F., Kato, T., Kawamiya, M., Knorr, W., Lindsay, K., Matthews, H., … Zeng, N. (2006). Climate-carbon cycle feedback analysis: Results from the C^4MIP model intercomparison. *Journal of Climate*, *19*, 3337–3353.

Girardin, M. P., Bouriaud, O., Hogg, E. H., Kurz, W., Zimmermann, N. E., Metsaranta, J. M., de Jong, R., Frank, D. C., Esper, J., Büntgen, U., Guo, X. J., & Bhatti, J. (2016). No growth stimulation of Canada's boreal forest under half-century of combined warming and CO_2 fertilization. *Proceedings of the National Academy of Sciences of the United States of America*, *113*, E8406–E8414.

Griffiths, N. A., Hanson, P. J., Ricciuto, D. M., Iversen, C. M., Jensen, A. M., Malhotra, A., McFarlane, K. J., Norby, R. J., Sargsyan, K., Sebestyen, S. D., Shi, X., Walker, A. P., Ward, E. J., Warren, J. M., & Weston, D. J. (2017). Temporal and spatial variation in peatland carbon cycling and implications for interpreting responses of an ecosystem-scale warming experiment. *Soil Science Society of America Journal*, *81*, 1668–1688.

Hanson, P. J., Gill, A. L., Xu, X., Phillips, J. R., Weston, D. J., Kolka, R. K., Riggs, J. S., & Hook, L. A. (2016). Intermediate-scale community-level flux of CO_2 and CH_4 in a Minnesota peatland: Putting the SPRUCE project in a global context. *Biogeochemistry*, *129*, 255–272.

Hanson, P. J., Griffiths, N. A., Iversen, C. M., Norby, R. J., Sebestyen, S. D., Phillips, J. R., Chanton, J. P., Kolka, R. K., Malhotra, A., Oleheiser, K. C., Warren, J. M., Shi, X., Yang, X., Mao, J., & Ricciuto, D. M. (2020). Rapid net carbon loss from a whole-ecosystem warmed peatland. *AGU Advances*, *1*, e2020AV000163.

Hanson, P. J., Riggs, J. S., Nettles, W. R., Phillips, J. R., Krassovski, M. B., Hook, L. A., Gu, L., Richardson, A. D., Aubrecht, D. M., Ricciuto, D. M., Warren, J. M., & Barbier, C. (2017). Attaining whole-ecosystem warming using air and deep-soil heating methods with an elevated CO_2 atmosphere. *Biogeosciences*, *14*, 861–883.

Hartmann, H., Bahn, M., Carbone, M., & Richardson, A. D. (2020). Plant carbon allocation in a changing world – Challenges and progress: Introduction to a virtual issue on carbon allocation. *New Phytologist*, *227*, 981–988.

Hou, E., Lu, X., Jiang, L., Wen, D., & Luo, Y. (2019). Quantifying soil phosphorus dynamics: A data assimilation approach. *Journal of Geophysical Research: Biogeosciences*, *124*, 2159–2173.

Huang, Y., Ciais, P., Luo, Y., Zhu, D., Wang, Y., Qiu, C., Goll, D. S., Guenet, B., Makowski, D., De Graaf, I., Leifeld, J., Kwon, M. J., Hu, J., & Qu, L. (2021). Tradeoff of CO_2 and CH_4 emissions from global peatlands under water-table drawdown. *Nature Climate Change*, *11*, 618–622.

Huang, Y., Jiang, J., Ma, S., Ricciuto, D., Hanson, P. J., & Luo, Y. (2017). Soil thermal dynamics, snow cover, and frozen depth under five temperature treatments in an ombrotrophic bog: Constrained forecast with data assimilation. *Journal of Geophysical Research: Biogeosciences*, *122*, 2046–2063.

Huang, Y., Lu, X., Shi, Z., Lawrence, D., Koven, C. D., Xia, J., Du, Z., Kluzek, E., & Luo, Y. (2018). Matrix approach to land carbon cycle modeling: A case study with the Community Land Model. *Global Change Biology*, *24*, 1394–1404.

Huang, Y., Zhu, D., Ciais, P., Guenet, B., Huang, Y., Goll, D. S., Guimberteau, M., Jornet-Puig, A., Lu, X., & Luo, Y. (2018). Matrix-based sensitivity assessment of soil organic carbon storage: A case study from the ORCHIDEE-MICT model. *Journal of Advances in Modeling Earth Systems*, *10*, 1790–1808.

Huntzinger, D. N., Michalak, A. M., Schwalm, C., Ciais, P., King, A. W., Fang, Y., Schaefer, K., Wei, Y., Cook, R. B., Fisher, J. B., Hayes, D., Huang, M., Ito, A., Jain, A. K., Lei, H., Lu, C., Maignan, F., Mao, J., Parazoo, N., … Zhao, F. (2017). Uncertainty in the response of terrestrial carbon sink to environmental drivers undermines carbon-climate feedback predictions. *Scientific Reports*, *7*, 4765.

Huntzinger, D. N., Schwalm, C., Michalak, A. M., Schaefer, K., King, A. W., Wei, Y., Jacobso, A., Liu, S., Cook, R. B., Post, W. M., Berthier, G., Hayes, D., Huang, M., Ito, A., Lei, H., Lu, C., Mao, J., Peng, C. H., Peng, S., … Zhu, Q. (2013). The north American carbon program multi-scale synthesis and terrestrial model intercomparison project – Part 1: Overview and experimental design. *Geoscientific Model Development*, *6*, 2121–2133.

IPCC. (2021). *Climate change 2021: The physical science basis. Contribution of Working Group I to the Sixth Assessment Report of the Intergovernmental Panel on Climate Change*. Cambridge University Press.

Jiang, L., Shi, Z., Xia, J., Liang, J., Lu, X., Wang, Y., & Luo, Y. (2017). Transient traceability analysis of land carbon storage dynamics: Procedures and its application to two forest ecosystems. *Journal of Advances in Modeling Earth Systems*, *9*, 2822–2835.

Keenan, T. F., & Williams, C. A. (2018). The terrestrial carbon sink. *Annual Review of Environment and Resources*, *43*, 219–243.

Kirschbaum, M. U. F., & Paul, K. I. (2002). Modelling C and N dynamics in forest soils with a modified version of the CENTURY model. *Soil Biology and Biochemistry*, *34*, 341–354.

Koven, C. D., Riley, W. J., Subin, Z. M., Tang, J. Y., Torn, M. S., Collins, W. D., Bonan, G. B., Lawrence, D. M., & Swenson, S. C. (2013). The effect of vertically resolved soil biogeochemistry and alternate soil C and N models on C dynamics of CLM4. *Biogeosciences*, *10*, 7109–7131.

Lee, J., Yoon, T., Han, S., Kim, S., Yi, M., Park, G., Kim, C., Son, Y. M., Kim, R., & Son, Y. (2014). Estimating the carbon dynamics of South Korean forests from 1954 to 2012. *Biogeosciences*, *11*, 4637–4650.

Liang, X., Zhang, T., Lu, X., Ellsworth, D. S., BassiriRad, H., You, C., Wang, D., He, P., Deng, Q., Liu, H., Mo, J., & Ye, Q. (2020). Global response patterns of plant photosynthesis to nitrogen addition: A meta-analysis. *Global Change Biology*, *26*, 3585–3600.

López-Blanco, E., Exbrayat, J. F., Lund, M., Christensen, T. R., Tamstorf, M. P., Slevin, D., Hugelius, G., Bloom, A. A., & Williams, M. (2019). Evaluation of terrestrial pan-Arctic carbon cycling using a data-assimilation system. *Earth System Dynamics*, *10*, 233–255.

Lopez-Blanco, E., Langen, P. L., Williams, M., Christensen, J. H., Boberg, F., Langley, K., & Christensen, T. R. (2022). The future of tundra carbon storage in Greenland – Sensitivity to climate and plant trait changes. *Science of the Total Environment*, *846*, 157385.

Lu, X., Du, Z., Huang, Y., Lawrence, D., Kluzek, E., Collier, N., Lombardozzi, D., Sobhani, N., Schuur, E. A. G., & Luo, Y. (2020). Full implementation of matrix approach to biogeochemistry module of CLM5. *Journal of Advances in Modeling Earth Systems*, *12*, e2020MS002105.

Luo, Y., Ahlström, A., Allison, S. D., Batjes, N. H., Brovkin, V., Carvalhais, N., Chappell, A., Ciais, P., Davidson, E. A., Finzi, A., Georgiou, K., Guenet, B., Hararuk, O., Harden, J. W., He, Y., Hopkins, F., Jiang, L., Koven, C., Jackson, R. B., … Zhou, T. (2016). Toward more realistic projections of soil carbon dynamics by Earth system models. *Global Biogeochemical Cycles*, *30*, 40–56.

Luo, Y., Huang, Y., Sierra, C. A., Xia, J., Ahlström, A., Hararuk, O., Hou, E., Jiang, L., Liao, C., Lu, X., Shi, Z., Smith, B., Tao, F., & Wang, Y.-P. (2022). Matrix approach to land carbon cycle modeling. *Journal of Advances in Modeling Earth Systems*, *14*, e2022MS003008.

Luo, Y., Randerson, J. T., Friedlingstein, P., Hibbard, K., Hoffman, F., Huntzinger, D., Jones, C. D., Koven, C., Lawrence, D., Li, D. J., Mahecha, M., Niu, S. L., Norby, R., Piao, S. L., Qi, X., Peylin, P., Prentice, I. C., Riley, W., Reichstein, M., … Li, D. (2012).

A framework for benchmarking land models. *Biogeosciences*, *9*, 3857–3874.

Luo, Y., & Schuur, E. A. G. (2020). Model parameterization to represent processes at unresolved scales and changing properties of evolving systems. *Global Change Biology*, *26*, 1109–1117.

Luo, Y., Shi, Z., Lu, X., Xia, J., Liang, J., Jiang, J., Wang, Y., Smith, M. J., Jiang, L., Ahlström, A., Chen, B., Hararuk, O., Hastings, A., Hoffman, F., Medlyn, B., Niu, S., Rasmussen, M., Todd-Brown, K., & Wang, Y.-P. (2017). Transient dynamics of terrestrial carbon storage: Mathematical foundation and its applications. *Biogeosciences*, *14*, 145–161.

Luo, Y., & Weng, E. (2011). Dynamic disequilibrium of the terrestrial carbon cycle under global change. *Trends in Ecology & Evolution*, *26*, 96–104.

Ma, S., Jiang, J., Huang, Y., Shi, Z., Wilson, R. M., Ricciuto, D., Sebestyen, S. D., Hanson, P. J., & Luo, Y. (2017). Data-constrained projections of methane fluxes in a northern Minnesota peatland in response to elevated CO_2 and warming. *Journal of Geophysical Research - Biogeosciences*, *122*, 2841–2861.

Manzoni, S., Čapek, P., Porada, P., Thurner, M., Winterdahl, M., Beer, C., Brüchert, V., Frouz, J., Herrmann, A. M., Lindahl, B. D., Lyon, S. W., Šantrůčková, H., Vico, G., & Way, D. (2018). Reviews and syntheses: Carbon use efficiency from organisms to ecosystems – Definitions, theories, and empirical evidence. *Biogeosciences*, *15*, 5929–5949.

Manzoni, S., & Porporato, A. (2009). Soil carbon and nitrogen mineralization: Theory and models across scales. *Soil Biology and Biochemistry*, *41*, 1355–1379.

McGuire, A. D., Melillo, J. M., Joyce, L. A., Kicklighter, D. W., Grace, A. L., Moore, B., & Vorosmarty, C. J. (1992). Interactions between carbon and nitrogen dynamics in estimating net primary productivity for potential vegetation in North America. *Global Biogeochemical Cycles*, *6*, 101–124.

Montané, F., Fox, A. M., Arellano, A. F., MacBean, N., Alexander, M. R., Dye, A., Bishop, D. A., Trouet, V., Babst, F., Hessi, A. E., Pederson, N., Blanken, P. D., Bohrer, G., Gough, C. M., Litvak, M. E., Novick, K. A., Philips, R. R., Wood, J. D., & Moore, D. J. P. (2017). Evaluating the effect of alternative carbon allocation schemes in a land surface model (CLM4.5) on carbon fluxes, pools, and turnover in temperate forests. *Geoscientific Model Development*, *10*, 3499–3517.

Nichols, J. E., & Peteet, D. M. (2019). Rapid expansion of northern peatlands and doubled estimate of carbon storage. *Nature Geoscience*, *12*, 917–921.

Potter, C. S., Randerson, J. T., Field, C. B., Matson, P. A., Vitousek, P. M., Mooney, H. A., & Klooster, S. A. (1993). Terrestrial ecosystem production: A process model-based on global satellite and surface data. *Global Biogeochemical Cycles*, *7*, 811–841.

R Core Team. (2020). *R: A language and environment for statistical computing*. R Foundation for Statistical Computing. http://www.R-project.org/

Rafique, R., Xia, J. Y., Hararuk, O., Asrar, G. R., Leng, G. Y., Wang, Y. P., & Luo, Y. Q. (2016). Divergent predictions of carbon storage between two global land models: Attribution of the causes through traceability analysis. *Earth System Dynamics*, *7*, 649–658.

Raich, J. W., Rastetter, E. B., Melillo, J. M., Kicklighter, D. W., Steudler, P. A., Peterson, B. J., Grace, A. L., Moore, B., 3rd, & Vorosmarty, C. J. (1991). Potential net primary productivity in South America: Application of a global model. *Ecological Applications*, *1*, 399–429.

Shi, Z., Allison, S. D., He, Y., Levine, P. A., Hoyt, A. M., Beem-Miller, J., Zhu, Q., Wieder, W. R., Trumbore, S., & Randerson, J. T. (2020). The age distribution of global soil carbon inferred from radiocarbon measurements. *Nature Geoscience*, *13*, 555–559.

Sierra, C. A., Ceballos-Nunez, V., Metzler, H., & Muller, M. (2018). Representing and understanding the carbon cycle using the theory of compartmental dynamical systems. *Journal of Advances in Modeling Earth Systems*, *10*, 1729–1734.

Smith, P., Soussana, J.-F., Angers, D., Schipper, L., Chenu, C., Rasse, D. P., Batjes, N. H., van Egmond, F., McNeill, S., Kuhnert, M., Arias-Navarro, C., Olesen, J. E., Chirinda, N., Fornara, D., Wollenberg, E., Álvaro-Fuentes, J., Sanz-Cobena, A., & Klumpp, K. (2020). How to measure, report and verify soil carbon change to realize the potential of soil carbon sequestration for atmospheric greenhouse gas removal. *Global Change Biology*, *26*, 219–241.

Tao, F., Zhou, Z., Huang, Y., Li, Q., Lu, X., Ma, S., Huang, X., Liang, Y., Hugelius, G., Jiang, L., Doughty, R., Ren, Z., & Luo, Y. (2020). Deep learning optimizes data-driven representation of soil organic carbon in Earth system model over the conterminous United States. *Frontiers in Big Data*, *3*, 17.

Tfaily, M. M., Cooper, W. T., Kostka, J. E., Chanton, P. R., Schadt, C. W., Hanson, P. J., Iversen, C. M., & Chanton, J. P. (2014). Organic matter transformation in the peat column at Marcell Experimental Forest: Humification and vertical stratification. *Journal of Geophysical Research: Biogeosciences*, *119*, 661–675.

Todd-Brown, K. E. O., Randerson, J. T., Post, W. M., Hoffman, F. M., Tarnocai, C., Schuur, E. A. G., & Allison, S. D. (2013). Causes of variation in soil carbon simulations from CMIP5 Earth system models and comparison with observations. *Biogeosciences*, *10*, 1717–1736.

Wei, N., Xia, J., Zhou, J., Jiang, L., Cui, E., Ping, J., & Luo, Y. (2022). Evolution of uncertainty in terrestrial carbon storage in Earth system models from CMIP5 to CMIP6. *Journal of Climate*, *35*, 1–33.

Wieder, W. R., Cleveland, C. C., Lawrence, D. M., & Bonan, G. B. (2015). Effects of model structural uncertainty on carbon cycle projections: Biological nitrogen fixation as a case study. *Environmental Research Letters*, *10*, 044016.

Xia, J., Luo, Y., Wang, Y. P., & Hararuk, O. (2013). Traceable components of terrestrial carbon storage capacity in biogeochemical models. *Global Change Biology*, *19*, 2104–2116.

Xia, J., Luo, Y., Wang, Y.-P., Weng, E., & Hararuk, O. (2012). A semi-analytical solution to accelerate spin-up of a coupled carbon and nitrogen land model to steady state. *Geoscientific Model Development*, *5*, 1259–1271.

Zhang, Y., Yu, G., Yang, J., Wimberly, M. C., Zhang, X., Tao, J., Jiang, Y., & Zhu, J. (2014). Climate-driven global changes in carbon use efficiency. *Global Ecology and Biogeography*, *23*, 144–155.

Zhou, J., Xia, J., Wei, N., Liu, Y., Bian, C., Bai, Y., & Luo, Y. (2021). A traceability analysis system for model evaluation on land carbon dynamics: Design and applications. *Ecological Processes*, *10*, 12.

Zhou, S., Liang, J., Lu, X., Li, Q., Jiang, L., Zhang, Y., Schwalm, C. R., Fisher, J. B., Tjiputra, J., Sitch, S., Ahlström, A., Huntzinger, D. N., Huang, Y., Wang, G., & Luo, Y. (2018). Sources of uncertainty in modeled land carbon storage within and across three MIPs: Diagnosis with three new techniques. *Journal of Climate*, *31*, 2833–2851.

SUPPORTING INFORMATION

Additional supporting information can be found online in the Supporting Information section at the end of this article.

How to cite this article: Hou, E., Ma, S., Huang, Y., Zhou, Y., Kim, H.-S., López-Blanco, E., Jiang, L., Xia, J., Tao, F., Williams, C., Williams, M., Ricciuto, D., Hanson, P. J., & Luo, Y. (2023). Across-model spread and shrinking in predicting peatland carbon dynamics under global change. *Global Change Biology*, *29*, 2759–2775. https://doi.org/10.1111/gcb.16643